Dynamics of counterions in dendrimer polyelectrolyte solutions

K. Karatasos[a] and M. Krystallis
Department of Chemical Engineering, Physical Chemistry Laboratory, Aristotle University of Thessaloniki, 54124 Thessaloniki, Greece

(Received 10 January 2009; accepted 1 February 2009; published online 17 March 2009)

Molecular dynamics simulations were employed in models of peripherally charged dendrimers in solutions of explicit solvent and monovalent counterions in order to explore aspects of the dynamic behavior of counterions. The present study explores the effects of varying strength of electrostatic interactions for models of two dendrimer generations, in explicit solvent solutions below the dendrimer overlap concentration. Counterion diffusional motion as well as residence lifetimes of pairs formed by charged dendrimer beads and condensed counterions is monitored in the different electrostatic regimes. Spatiotemporal characteristics of self- and collective counterion motion are explored by means of space-time Van Hove correlation functions. A characteristic scaling law is found to describe the counterion diffusion coefficient as a function of Bjerrum length in the strong electrostatic regime, independent of the size of the dendrimer molecules at the examined volume fractions. The change noted in the diffusional motion of counterions in the range of strong Coulombic interactions is also reflected to their relevant residence times. Development of dynamic heterogeneities in counterion self-motion is observed during the gradual increase in the strength of electrostatic interactions, characterized by the emergence of distinct counterion populations in terms of their mobility. The time scale for the development of such a mobility contrast in the self-motion of the counterions can be correlated with that describing their collective motion as well. The latter increases with Bjerrum length but remains shorter compared to the time scale at which free diffusional motion sets in. Findings from the present study provide further insight on the mechanisms pertinent to ion migration in macroion dispersions and may serve as a basis for the interpretation of ionic motion in a broader range of polyelectrolyte systems. © *2009 American Institute of Physics*. [DOI: 10.1063/1.3088849]

I. INTRODUCTION

Understanding of the dynamic characteristics of the ionic atmosphere in the vicinity of charged macromolecular systems of industrial[1,2] or biological significance[3,4] is a crucial step for the interpretation of their physical behavior and ultimately toward the control of their properties. Issues such as spatial[5,6] and temporal[7,8] correlations between counterions, their self- and collective motion,[9,10] and the dynamics associated with the counterion condensation process[11] play a key role in phenomena such as the self-assembly of macromolecular systems,[12,13] the formation of complexes between biological molecules,[14,15] the counterion-mediated attraction between like-charged macroions and their possible under- or overcharging,[10,13,16–18] the stability of colloidal dispersions and polymeric gels,[19–21] etc.

Recent experimental,[4,8,22–24] theoretical,[25] and computational[11,26] studies revealed that the characteristic time scales involved in counterion dynamics in polyelectrolyte systems may span several orders of magnitude ranging from subnanosecond times to time scales corresponding to acoustic frequencies.[27] These characteristic times describing self- or collective counterion motions were found to be directly associated with the details of their spatial arrangement around the macroions.[27] Depending on the strength of the electrostatic interactions, it has been found[28,29] that distinct "phases" of counterions can be formed, i.e., a "condensed" and a "diffuse" phase consisting of the tightly and the loosely bound counterions to the considered macroion, respectively. These phases are considered transient rather than permanent with a constant dynamic exchange of counterions between them.[8,11,30,31] Dynamic modes arising from correlated motion of counterions located at a close proximity[10,11,32] to the macroion or even in the diffuse phase[31,33,34] may actually induce conformational changes to the macroion, while collective motion of the more mobile ions can be involved in the formation of charge density waves[10] which may trigger macroion self-assembly.

To all the above dynamic processes, the internal structure of the charged macroion can be of particular importance. Possibility of interpenetration or even entrapment of counterions within the macroion's interior,[35] solvent, or ion depletion phenomena which may influence the thermodynamics of the system[13,36,37] should be explicitly accounted for. Other parameters relevant to the dynamic behavior of the counterions include their valency, the strength of electrostatic interactions (associated, e.g., with the ionic strength of the solution, the dielectric permittivity of the solvent, or the existence of an external electromagnetic field), and the concentration of the macroions.[11,22,25,38]

In this work we study the dynamic behavior of counte-

[a]Author to whom correspondence should be addressed. Electronic mail: karatas@eng.auth.gr.

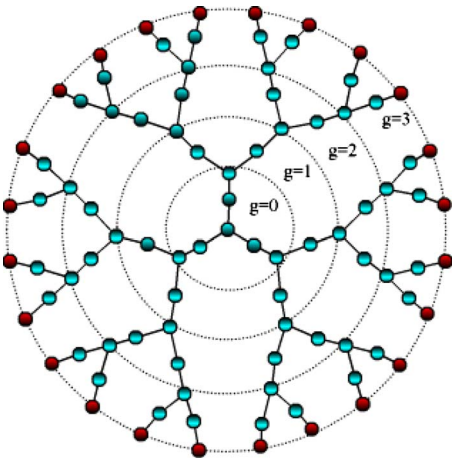

FIG. 1. (Color online) A schematic of the topology of a third generation dendrimer (G3). The concentric circles denote the boundaries of the generational shells. The terminal charged beads are shown in different colors.

rions in systems comprised by dendritic molecules of two different sizes (generations) in explicit solvent solutions in the dilute regime, subjected to a varying strength of electrostatic interactions. We have also invoked two different dendrimer concentrations for models of each generation in order to check for possible box size or total volume fraction effects. The strength of electrostatic interactions examined covers a range from a weak Coulombic regime in which only a liquidlike ordering of the dendrimer molecules and the counterions is present to a strong electrostatic regime in which counterion condensation takes place and the dendrimer molecules self-organize in cubic phases.[13] Experimentally such conditions of varying strength of electrostatic interactions can be realized, e.g., by modifying the Bjerrum length of the solution via appropriate choice of the solvent's dielectric permittivity.[39–41]

Due to their dense branching pattern and their well defined dimensions (low polydispersity), dendrimer molecules essentially bear characteristics of polymeric as well as of colloidal nature.[42] We therefore believe that the results from the present study may serve as a basis for the description of a broader category of materials including systems of globular proteins, spherical brushes, and colloidal dispersions.

II. MODEL DESCRIPTION AND SIMULATION DETAILS

Four systems of terminally charged dendrimers in an atomistic (united atom) representation together with the corresponding number of neutralizing counterions and explicit solvent beads were simulated by means of molecular dynamics (MD) simulations in the constant-temperature constant-volume (*NVT*) ensemble. The structure of the dendritic molecule considered starts from a trifunctional core and grows radiallly outward with two bonds intervening between branching points,[43] as illustrated in Fig. 1

The maximum number of generational shells (see Fig. 1) denotes the generation of the dendrimer. In this work systems of generations 3 (denoted as G3) and 4 (denoted as G4) were studied. Each system was comprised by 30 dendrimer molecules. The characteristics of the models examined (i.e., number of counterions and solvent beads) are listed in Table I. In all the examined models the dendrimer concentration (C) remained below the overlap limit (C^*). Variation in the strength of electrostatic interactions was realized by modifying the Bjerrum length (l_B).[13] The simulation protocol followed included successive steps of energy minimization and *NVT* MD cycles utilizing the DREIDING (Ref. 44) force field for equilibration of the constructed models.

TABLE I. Details on the composition of the simulated systems. C represents the dendrimer concentration and C^* the corresponding dendrimer overlap limit.

System code	G3_1	G3_2	G4_1	G4_2
Generation	3	3	4	4
C/C^* of dendrimer	0.10	0.07	0.09	0.06
Number of counterions	720	720	1440	1440
Number of solvent beads	1086	1629	2300	6534
Total volume fraction[a]	0.44	0.33	0.36	0.36

[a]In the calculations of total volume fraction, the volume of dendrimers, counterions, and solvent beads is taken into account.

Force field terms included bonded (bond stretching, angle bending, and torsional angles' rotation) and nonbonded (van der Waals and Coulombic) interactions. The electrostatic interactions between charged beads were accounted for by full Ewald summation, while no attractive part was considered in the van der Waals interaction between two charged beads. The adopted simulation procedure and all the relevant parameters are described in detail in our previous work.[13] The unit of length is taken equal to σ (the Lennard-Jones parameter between two charged beads), while time is expressed in units of τ (the characteristic time of our model) which corresponds to approximately 1.4×10^3 MD steps.[13]

III. THE ELECTROSTATIC REGIMES

As was described in our earlier study for systems G3_1 and G4_1 (see Ref. 13, Fig. 7), depending on the strength of electrostatic interactions, three distinct regimes could be distinguished based on characteristic changes in the static behavior of the dendrimer molecules: (i) a weak electrostatic region (quoted in Ref. 13 as regime I) in which the spatial arrangement of dendrimer molecules remained insensitive to Bjerrum length changes, (ii) an intermediate electrostatic regime (quoted in Ref. 13 as regime II) over which a stronger Coulombic coupling between the charged objects was realized leading to a gradual counterion condensation and self-ordering of the dendrimer molecules, and regime III at the higher l_B values examined ($l_B/\sigma>60$), within which the dendrimers remained in an ordered structure with practically the entire population of counterions located in their close vicinity. The same picture characterized by the aforementioned electrostatic regimes describes the G3_2 and G4_2 systems as well (figures describing their static behavior are not shown here). In this work, we will mainly discuss the dynamic behavior of counterions over Bjerrum lengths up to $l_B/\sigma=60$, so that the longer relevant time scales reside within our simulation window.

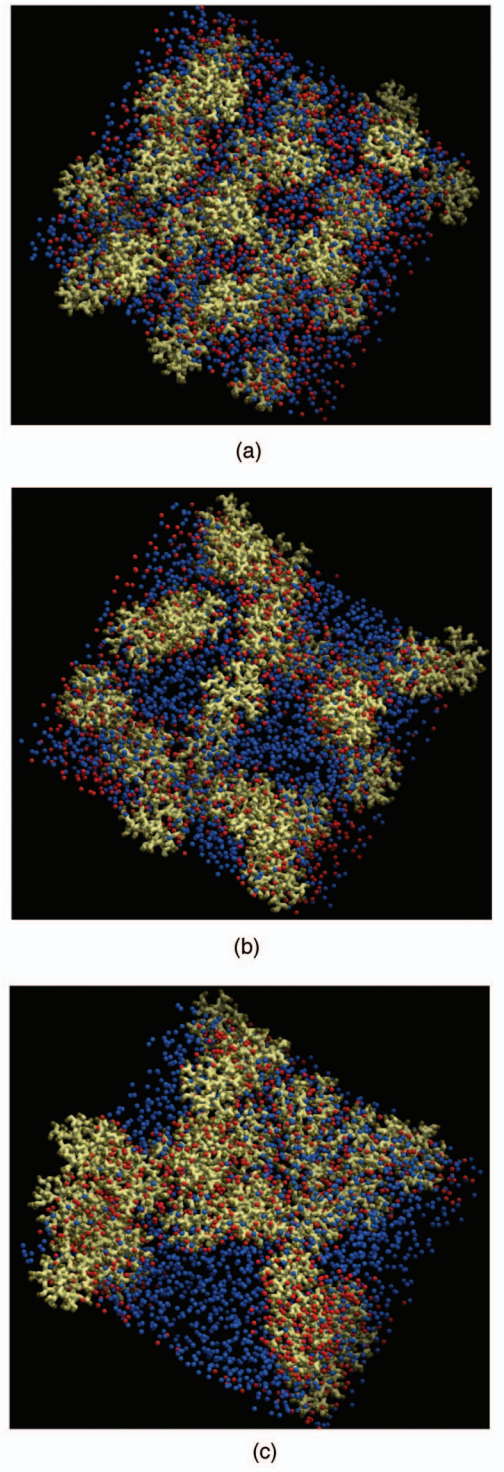

FIG. 2. (Color) Snapshots of system G4_1 at three different values of Bjerrum length (a) $l_B/\sigma=1$, (b) $l_B/\sigma=10$, and (c) $l_B/\sigma=60$. Solvent beads are shown in blue and counterions in red.

Figure 2 shows snapshots of one of the examined systems (representative for all the models studied) at three Bjerrum lengths, where the different degrees of counterion condensation can be visually recognized. In Fig. 2(a) counterions are practically homogeneously dispersed, in Fig. 2(b) populations of condensed and noncondensed counterions can be identified, while in Fig. 2(c) almost the entire population of the counterions appears to be bound on dendrimer molecules.

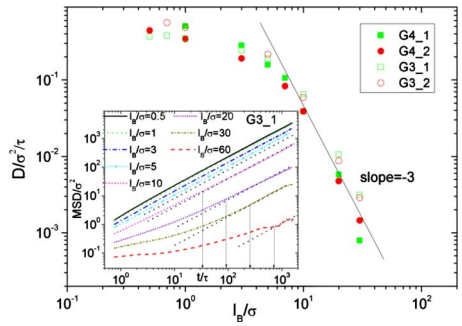

FIG. 3. (Color online) Main panel: Diffusion coefficients of the counterions as a function of l_B for all the studied models. The solid line indicates a slope of -3. Inset: Mean squared displacement of the counterions at different Bjerrum lengths for one of the examined models. The thick dotted lines denote a slope of 1. The arrows mark the residence times of counterions as will be discussed in Sec. VI.

IV. TRANSLATIONAL MOTION

To explore the effects of the variation in the strength of electrostatic interactions on the translational motion of counterions, we have monitored their mean square displacement (MSD) as a function of time. At all the systems, diffusion of counterions has reached the hydrodynamic limit at $l_B/\sigma \leq 60$. Diffusion coefficients were calculated from the long-time limit behavior of the MSD (see e.g., Fig. 3, inset) according to

$$D = \frac{1}{6}\lim_{t\to\infty}\frac{d}{dt}\langle|\boldsymbol{R}(t)-\boldsymbol{R}(0)|^2\rangle, \tag{1}$$

where $\boldsymbol{R}(t)$ represents the position vector of a counterion at time t. The angle brackets denote both time and ensemble average. Figure 3 shows the dependence of the diffusion coefficients upon variation of Bjerrum length.

Although no significant differences are observed between the diffusion coefficients of systems of the same dendrimer generation (i.e., between G3_1 and G3_2 and between G4_1 and G4_2), in smaller size models counterion diffusion appears somewhat faster. At low Bjerrum lengths, a rather weak variation in the diffusion coefficient characterizes counterion motion. In contrast, when Coulombic interactions grow larger, diffusional motion undergoes a dramatic slowdown apparently following a strong power-law dependence on Bjerrum length. In particular, it appears that an exponent of -3 provides a fair description of all data in this regime.

In order to better understand the observed behavior, it is informative to examine the diffusional motion of the dendrimer molecules themselves, since at high l_B values counterions are to a large extent[13] condensed on the dendrimer molecules and thus are expected to follow closely the dendrimers' translational motion.

Figure 4 depicts the dependence of the diffusion coefficient of the center of mass of the dendrimer molecules on Bjerrum length. An example of the MSD describing the center of mass motion for one of the systems is shown as an inset. The main features observed in the counterion diffusional behavior of Fig. 3 are also present in the dendrimers' translational motion. The weak variation in the dendrimer

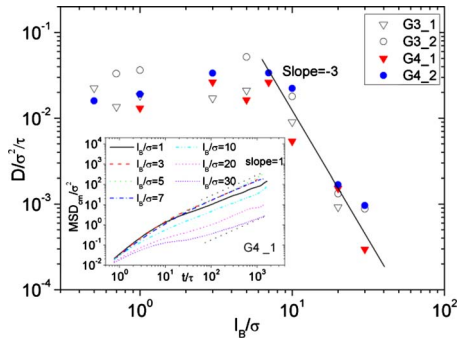

FIG. 4. (Color online) Main panel: Diffusion coefficient of the center of mass of the dendrimer molecules as a function of Bjerrum length. The solid line indicates a slope of −3. Inset: MSD of the center of mass of dendrimers for one of the studied systems. The thick dotted lines denote a slope of 1.

diffusion coefficient in the low l_B regime is followed by a marked drop upon increase in the strength of electrostatic interactions. Such a retardation of the center of mass motion (note the formation of a plateau in the corresponding MSD shown in the inset of Fig. 4 at the larger l_B value) is reminiscent of an analogous dynamic slowing down close to the glass transition observed in a wide range of systems, such as glass-forming liquids and polymers,[45] colloids,[46] and dendrimers.[47]

More specifically, in colloidal systems and, in particular, in the case of charge-stabilized colloidal suspensions, a dynamic anomaly in the diffusion coefficient as a function of the strength of Coulombic interactions has theoretically been predicted.[48] According to this study, correlations among the charged colloids and the counterions were found responsible for a significant slow down of the translational motion of the former, close to a characteristic volume fraction φ_g of the solute (the subscript g refers to a glasslike behavior). This characteristic volume fraction for highly charged colloidal systems was found to strongly decrease upon increase in l_B. In other words, an increase in l_B would bring the system much closer to a motionally "frozen" state imparting a marked drop in the colloid diffusional motion, in qualitative agreement to the dendrimers' behavior (Fig. 4). Since at that electrostatic regime most of the counterions are condensed on the dendrimer molecules[13] as stated earlier, it is reasonable to conclude that the same behavior will also characterize the diffusion of counterions (Fig. 3).

V. SPACE-TIME CORRELATED MOTION

A way to explore both collective as well as self-motions at different time scales is by probing the time dependence of the so-called Van Hove correlation function[49] $G(\boldsymbol{r},t)$ defined as

$$G(\boldsymbol{r},t) = \frac{1}{N}\left\langle \sum_i \sum_j \delta[\boldsymbol{r} + \boldsymbol{r}_i(0) - \boldsymbol{r}_j(t)] \right\rangle, \tag{2}$$

where N is the total number of particles, δ represents the Dirac's function, while $\boldsymbol{r}_i(t)$ is the position vector of the i_{th} particle at time t. This function is proportional to the probability that a particle is at position $\boldsymbol{r}$ at time t given that a particle was at the origin ($\boldsymbol{r}=0$) at time $t=0$. Its Fourier transform can be probed by experimental techniques possessing space-time resolution capabilities such as neutron scattering,[50] in order to extract dynamic structure information. By separating the $i=j$ and the $i \neq j$ terms in Eq. (2), the Van Hove correlation function can be expressed as a sum of a self- and a distinct part $G(\boldsymbol{r},t)=G_s(\boldsymbol{r},t)+G_d(\boldsymbol{r},t)$. The self-part for homogeneous uniform substances can be expressed as

$$G_s(r,t) = \frac{1}{N}\left\langle \sum_i \delta[r - |\boldsymbol{r}_i(t) - \boldsymbol{r}_i(0)|] \right\rangle, \tag{3}$$

where r symbolizes the distance between the positions of the i_{th} particle at times t and 0. It probes self-motion as a function of time and is related via its Fourier transform to the *incoherent* dynamic structure factor probed by scattering experiments. In analogy, the distinct part is given by

$$G_d(r,t) = \frac{1}{N}\left\langle \sum_i \sum_{j \neq i} \delta[r - |\boldsymbol{r}_i(t) - \boldsymbol{r}_j(0)|] \right\rangle \tag{4}$$

and essentially probes collective dynamics at different length scales (its Fourier transform is associated with the *coherent* dynamic structure factor). In order to get a more detailed account regarding the motional mechanisms associated with counterion dynamics, we will present the self- and distinct parts separately.

A. Self-motion

As has been documented in past studies of local motion in glass-forming liquids,[51] ionic and metallic glasses,[52,53] or polymers,[54,55] $G_s(r,t)$ is a particularly sensitive probe in characterizing particles' motion in terms of their relative mobility. If all the particles monitored follow a free-of-obstacles homogeneous motion, the distances they travel at a specific time interval are Gaussian distributed and the self-Van Hove function varies as $G_s(r,t) \propto \exp[-3r^2/2\langle \Delta r^2(t) \rangle]$. In cases, however, where the homogeneous nature of their motion is inhibited, deviations from the Gaussian behavior are observed,[55] which under certain conditions may grow sufficiently strong to result in the formation of particle populations with distinctly different mobilities. This instance is directly reflected to the self-part of the Van Hove function, since particles possessing distinct mobilities travel different distances at specific time periods.

As has been discussed in our previous work,[13] increase in the strength of electrostatic interactions results to a growing degree of counterion condensation, enhancing at the same time the mobility contrast between the condensed and the "loose" counterions around the charged dendrimers. It is therefore expected that for a specific time period, the distances spanned from counterions belonging to these two populations would depend on the Bjerrum length of the examined system. An example of the link between the level of electrostatic interactions and the time scale at which a noticeable dynamic contrast between counterions is developed, is illustrated in Fig. 5, where $4\pi r^2 G_s(r,t)$ for two of the examined models is shown at constant time but varying l_B. For both dendrimer size systems and for the particular time scale considered, only close to a specific l_B value (l_B/σ

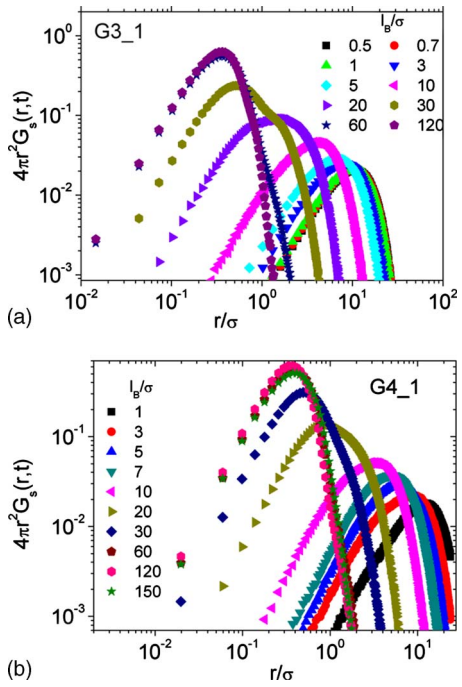

FIG. 5. (Color online) Self-Van Hove correlation functions for two of the examined models at a constant time scale $t \cong 77\tau$ but varying Bjerrum lengths. G3_1 (a) and G4_1 (b). At that time scale, indications for the development of a second peak appear at $l_B/\sigma = 30$.

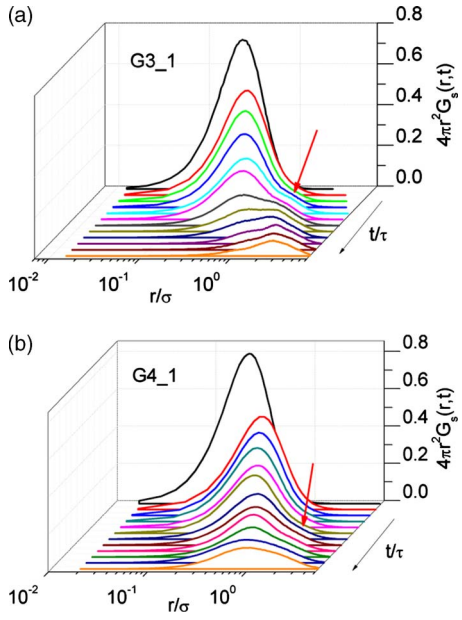

FIG. 6. (Color online) Self-Van Hove correlation functions (after angular integration) for two of the examined models at $l_B/\sigma = 30$ representing systems of generations 3 [G3_1, (a)] and 4 [G4_1, (b)]. The plotted curves cover time scales from 0.8τ to 769.2τ (0.8τ, 7.8τ, 15.4τ, 30.8τ, 61.5τ, 76.9τ, 153.8τ, 230.8τ, 307.8τ, 461.5τ, 615.4τ, and 769.2τ in sequence of appearance). The arrows point out the first appearance of a shoulder in the correlations functions.

$= 30$) a separation in the traveled distances (i.e., development of a second peak) becomes noticeable. At larger values of Bjerrum length where most of the counterions become strongly bound to the dendrimers,[13] no clear indication of distinct counterion populations in terms of the spanned distances (i.e., indication of an additional peak) can be observed at the examined time scale.

This is also the case (i.e., the absence of a second peak) for Bjerrum lengths in the weak Coulombic regime, not only at the time scale specified in Fig. 5 but also at any time scale checked within the simulated trajectory length.

Figure 6 shows the time evolution of the self Van Hove function at a Bjerrum length value within the strong electrostatic regime.

As illustrated in the time evolution of the angular integrated self-Van Hove functions, a "shoulder" develops at time scales of the order of few tenths of the time unit. This shoulder grows in amplitude (more prominent in the G3 model) at larger time scales (of the order of 100τ and longer). The widest detectable separation in length scales spanned by the less and the more mobile counterions is between 2σ and 3σ.

Apart from the strength of the Coulombic coupling and the time scale examined, another parameter that should be taken into account when transport properties of counterions are to be examined is the concentration of the solute, i.e., that of the oppositely charged polyelectrolyte molecules.[22,26,56]

Figure 7 shows the dependence of self-Van Hove spectra on dendrimer concentration at constant Bjerrum length but different time periods.

At short time scales and for constant dendrimer size, $G_s(r,t)$ curves are practically indistinguishable between systems at different concentrations. At longer time scales, however, the separation of the traveled distances between systems at different concentrations becomes appreciable (note the relative shift of the curves as a function of time). The distances covered by counterions are expected to be larger at lower concentrations; this can be ascribed to the wider separations between nonbound counterions and dendrimers, al-

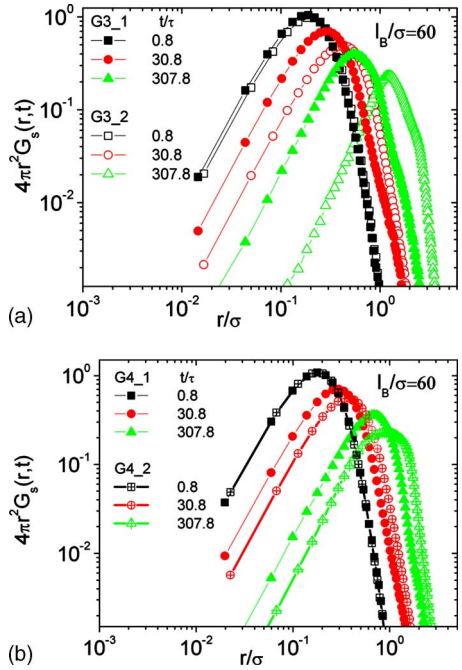

FIG. 7. (Color online) Comparison of $G_s(r,t)$ functions of counterions at constant $l_B/\sigma = 60$ for different time scales and for the systems at different dendrimer concentrations. (a): G3 models. (b): G4 models.

lowed by the availability of more space away from dendrimer molecules and therefore of more sites within the solution with relatively reduced Coulombic interactions. During the calculation of $G_s(r,t)$ no distinction is made between condensed and noncondensed counterions. However, the behavior observed in Fig. 7 can better be justified if we assume that it arises mainly from motion of noncondensed counterions.

B. Collective motion

The collective motion of counterions was explored by examining the distinct Van Hove correlation function [Eq. (4)], which essentially probes density fluctuations due to the collective motion of the neighbors around each particle. At the static case ($t=0$), the distinct Van Hove function is proportional to the radial distribution function $g(r)$, $G_d(r,0)=\rho g(r)$, where ρ represents the density. At large times and long separations the position of each particle is unrelated to the earlier position of another atom, so that $G_d(r,t)$ tends to a constant value, i.e., the average density of the system. Figure 8 demonstrates this behavior for $G_d(r,t)$ of one of the systems (G3_2) at different Bjerrum lengths (the behavior observed is representative for the other systems as well).

At the weak electrostatic regime [Fig. 8(a)] the peaks of $G_d(r,t)$ are smeared out after only a short period ($t\sim\tau$). As the Bjerrum length increases, the amplitude of the maxima decreases with a much lower rate, indicating a longer lasting "memory" of the initial (i.e., at $t=0$) arrangement of counterions. The gradual loss of this memory as times lapses originates from the collective motion of counterions. The time period up to which the peaks remain discernible as features of $G_d(r,t)$ can be taken as a measure of the characteristic time scale for the decay of the correlated motion of the counterions. To get an estimation of this time scale, we have defined the function

$$C(t)=\frac{G_d(r,t)-G_d(r,t^*)}{G_d(r,0)-G_d(r,t^*)}, \tag{5}$$

where t^* represents the time scale at which the peak corresponding to the first neighbor shell has practically been smeared out. Since at the weak electrostatic regime such a function would have decayed rapidly, we will focus only on larger Bjerrum length values.

Figure 9 shows $C(t)$ functions in semilogarithmic format for all the models examined. A direct visual inspection reveals that the long-time behavior of the logarithm of this function is to a good approximation linear in time, i.e., the pertinent dynamic process can be described by an exponential $C(t)\propto e^{-t/\tau_c}$, where τ_c can be identified as a characteristic time for the decay of $C(t)$. Moreover, $C(t)$ appears to be dependent on Bjerrum length; the larger the l_B the lower (in absolute value) the slope, i.e., the longer the characteristic time τ_c. By fitting straight lines in the semilogarithmic plots shown in Fig. 9 (the first point at the lower t/τ is excluded from the fit), we have estimated the characteristic decay times as plotted in Fig. 10

The characteristic time τ_c appears to increase with concentration, Bjerrum length, and dendrimer size. The increase

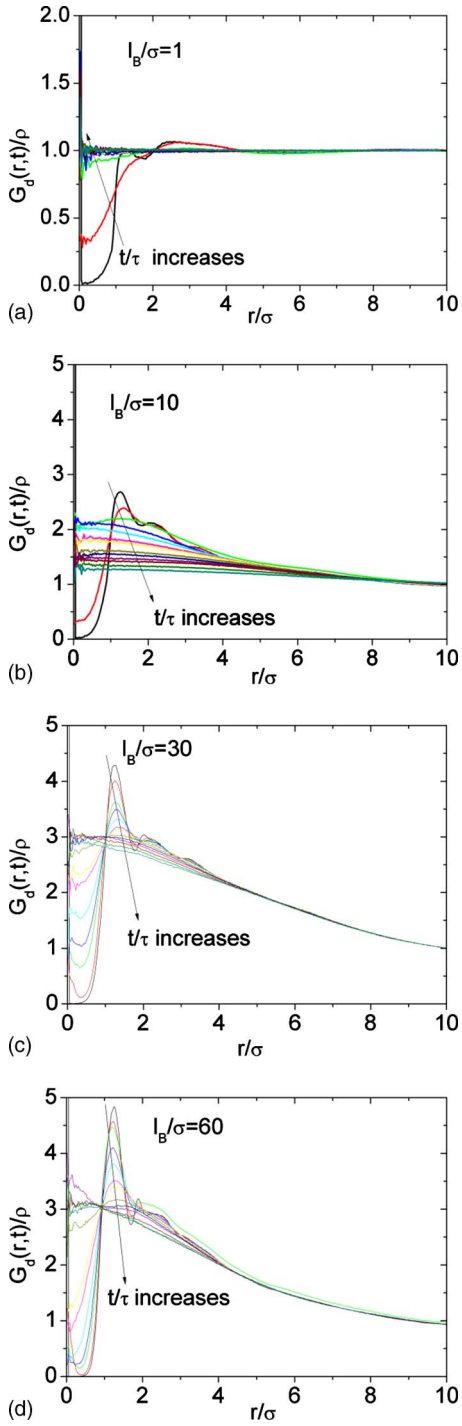

FIG. 8. (Color online) Distinct Van Hove correlation functions for system G3_2 at different Bjerrum lengths. The behavior observed in the rest of the examined systems is similar. Different curves in each plot correspond to different times. The arrows indicate the direction of increase in the time interval. The lowest time corresponds to the static case ($t/\tau=0$), while the longer times follow the same sequence as in Fig. 6.

in τ_c upon increase in concentration can be related to the analogous slowing down of individual counterion motion as was noted in the behavior of the self-part of the Van Hove function (Fig. 7). The same reason (retardation of self-motion) may also account for the observed dependence on Bjerrum length, since the diffusional motion of counterions was shown to slow down (Fig. 3) upon increase in l_B. The dependence on dendrimer size implies a coupling mechanism

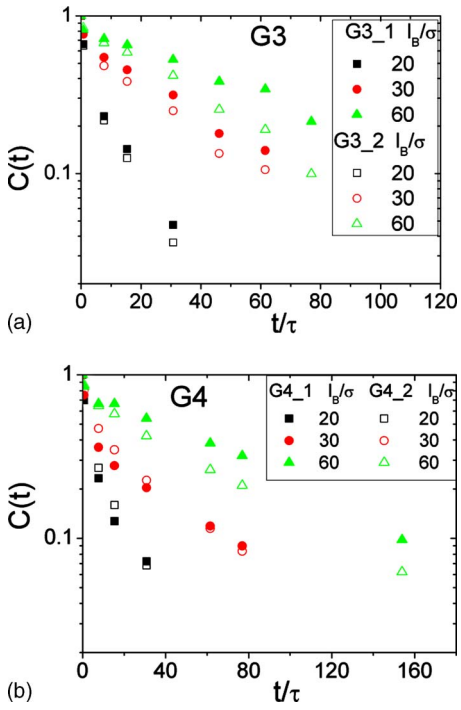

FIG. 9. (Color online) Semilogarithmic plots of $C(t)$ [Eq. (5)] for the G3 (a) and the G4 (b) models.

between dendrimer motion and collective counterion modes as these are probed by $C(t)$. This point will be revisited later on, after some further aspects of counterion dynamics have been discussed.

VI. DYNAMICS OF BOUND COUNTERIONS

In the examination of the self- and collective motion of counterions as described by the Van Hove functions, no distinction has been made between condensed and noncondensed populations. In order to relate the above discussed time scales to specific dynamic mechanisms, it would be informative to obtain a more detailed account on the behavior of distinct counterion populations. To this end, we have examined the residence time of the counterions bound to oppositely charged dendrimer beads by calculating the "survival time" correlation function defined as[57]

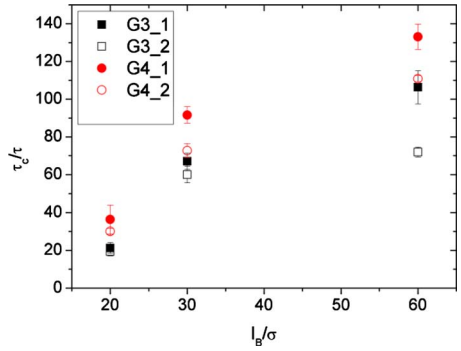

FIG. 10. (Color online) Characteristic times corresponding to the long-time behavior of $C(t)$ from Fig. 9, at the strong electrostatic regime.

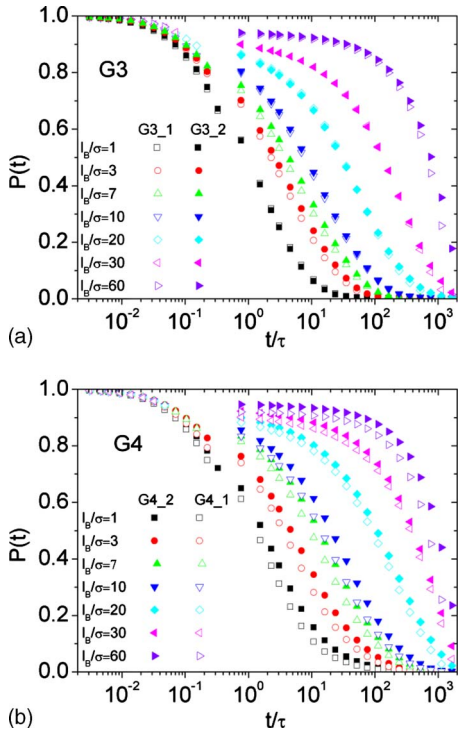

FIG. 11. (Color online) Survival time correlation functions for counterion-charged dendrimer bead pairs for the G3 (a) and the G4 (b) models at different Bjerrum lengths.

$$P(t) = \frac{\Sigma_{(i,j)} p_{ij}(t)}{\Sigma_{(i,j)} p_{ij}(t=0)}. \tag{6}$$

Here $p_{ij}(t)$ takes the value of 1 if a pair between a counterion and a terminal dendrimer bead (denoted with indices i and j) that exists at $t=0$ survives at time $t>0$, and 0 otherwise. A charged dendrimer bead and a counterion are considered to form a pair at time t, if their distance at that time is shorter than the separation corresponding to the first minimum of the relevant pair distribution function. For all the examined systems this minimum was approximately $r_{\text{cut}} \cong 1.6\sigma$ (see Supplementary Material).[58]

Figure 11 depicts the behavior of $P(t)$ for all the studied models at values of Bjerrum length covering different electrostatic regimes. In all models, increase in the strength of electrostatic interactions significantly affects the decay time of the correlation functions as anticipated, since an increase in Coulombic attraction naturally prolongs the period within which the initially formed pairs remain at a close proximity.

A visual inspection of the graphs shows that at constant dendrimer size, the curves corresponding to different concentrations differ only slightly. An average residence time τ_s can be estimated by integrating the survival correlation function, i.e., $\tau_s = \int_0^\infty P(t)dt$. The so-calculated average residence times are presented in Fig. 12. Apparently, the dependence of residence times on the strength of electrostatic interactions follows a common pattern in all the examined models. Apart from the effect of size and the minor shift in times due to concentration, both size models exhibit similar changes as a function of Bjerrum length.

Residence times seemingly follow a power-law dependence, which changes exponent (i.e., slope) above a thresh-

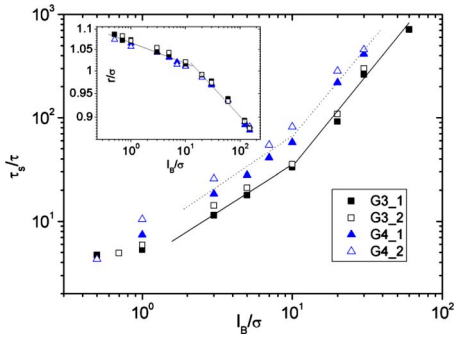

FIG. 12. (Color online) Residence times of counterion-charged bead pairs. The lines are guides to the eye. Inset: Dependence of the separation between counterions and charged dendrimer beads on Bjerrum length, as determined from the first neighbor peak of the corresponding pair distribution functions. Lines are guides to the eye.

old in l_B, signifying a dynamic transition. An analogous behavior characterizes the average separation between the two charged species as a function of Bjerrum length (inset of Fig. 12), indicating a close connection between the spatial arrangement of counterions and the character of their dynamic coupling with the charged dendrimer beads.

A close analogy of such a dynamic association between counterions and charged macroions from the experimental point of view can be found in the description of dielectric and birefringence experiments in polyelectrolyte solutions. In experiments conducted in solutions of linear polyelectrolytes[33] or linear micelles[32] in the presence of counterions, two principal mechanisms associated with counterion dynamics were identified. One, termed as the high frequency "HF" process,[32] was ascribed to the motion of weakly associated counterions perpendicular to the contour of the oppositely charged linear macroions, and another, slower dynamic mode (i.e., at a lower frequency window) termed as "LF." From the birefringence experiments[33] it was shown that the time scale of the LF process (although somewhat faster) was very close to that corresponding to the rotational relaxation motion of the macroions, i.e., to a mechanism related to global macroion dynamics.

Based on the above picture, we can surmise that the dynamic transition observed in the counterion residence times in our systems (Fig. 12) is due to the change in the nature of the counterions' motion with respect to dendrimer molecules: at a low strength of electrostatic interactions the counterions located close to the dendrimers are only weakly bound to them, performing a motion analogous to the HF process observed in dielectric experiments as described above. At higher l_B values, however, where the larger percentage of counterions becomes tightly bound to the dendrimers, their motion can become strongly coupled to the slower global dendrimer dynamics (e.g., dendrimer reorientation and/or translation), in analogy to the mechanism which gives rise to the LF process in birefringence experiments. Such a strong coupling between global dendrimer motion (translational and/or rotational) and counterions suffices to rationalize the dendrimer size dependence of the residence times at the strong electrostatic regime. On the other hand, in the weak Coulombic regime a molecular-size dependence of the residence times of counterions performing a HF-like motion could be introduced mainly via a coupling to the rotational motion of the dendrimer which can be considerably faster than the overall diffusion in dilute solutions.[43]

To check the consistency of the above arguments at least in the strong electrostatic regime, we can compare the time scale of the residence times with that corresponding to the onset of free diffusion of counterions. As the LF-like motion is the slower dynamic process involving counterions and since it refers to the majority of them at the high l_B range, it should essentially determine the time scale for their long-time diffusive behavior as well. Indeed, as shown in the inset of Fig. 3 for one of the examined models (the behavior of the other models is similar), the long-time diffusional motion of counterions sets in (i.e., a slope of 1 is attained) at a time scale only slightly longer compared to that associated with the respective average residence times (the arrows indicate the residence times corresponding to the specific model presented in Fig. 3).

VII. DISCUSSION

A direct comparison between the time scales characterizing the average residence period of the condensed counterions (Fig. 12) and that corresponding to the collective motion described by the distinct Van Hove function (Fig. 10) reveals that the latter are almost one order of magnitude shorter compared to the former. Since the time scale of collective counterion motion is realized at a considerably shorter time scale, motion of condensed counterions might in principle contribute to the relaxation of $C(t)$. However, at the strong electrostatic regime the condensed counterions become increasingly more localized in the vicinity of dendrimer molecules as it can be inferred by the increase in the height of the principal peak in the relevant pair correlation function (see Supplementary Material) and the decrease in the pair separation shown in Fig. 12, inset. Since they remain at that close proximity to charged dendrimer beads for much longer a period compared to the time scale for the relaxation of $C(t)$, we can consider that the contribution of the strongly bound population to counterion density fluctuations probed by $G_d(r,t)$ is practically negligible. It can therefore be inferred that dynamics monitored by $C(t)$ arises mainly due to the motion of the less constricted counterions. As indicated by the appearance of additional peaks in the pair distribution function (see Supplementary Material) counterions form next-neighbor diffuse shells around the dendrimers and around the strongly bound population. The separation between the first and the second peak in the pair distribution function at large l_B values, representing the condensed and the next diffuse counterion layer respectively, is approximately 1.2σ (see Supplementary Material). This separation is consistent with the location of the first peak in the counterion-counterion pair distribution function in the strong electrostatic regime (see Fig. 12 in Ref. 13) and with the location of the peak monitored by $G_d(r,t)$ (see Fig. 8). In other words, it appears reasonable to relate the dynamics probed by $C(r,t)$ in the strong electrostatic regime to the

collective motion of counterions belonging in principle to the second neighbor shell around the dendrimer molecules.

The above described picture allows us to elaborate more on the characteristics of the self-motion of counterions as described by the self-part of the Van Hove correlation function. As was illustrated in Fig. 6, for an l_B value in the strong electrostatic regime the time scale associated with the first appearance of a shoulder or a second peak in $G_s(r,t)$ is much shorter compared to the residence time at the same Bjerrum length (compare to the times corresponding to $l_B/\sigma=30$ for models G3_1 and G4_1 as shown in Fig. 12), but only marginally shorter compared to the respective time scale for the collective counterion motion as probed by $C(t)$ (see the times for the same l_B value in Fig. 10). On these grounds, a direct link can be established between the time scale for the buildup of a sufficiently high self-motion contrast among the tightly and loosely bound counterions and the time scale associated with the collective motion of the latter.

A mechanism which may contribute to the development of such a dynamic contrast between counterions located close to the dendrimer periphery is the so-called "hopping" mechanism which has been identified in biological systems[59] in polymer electrolyte solutions[60,61] and in disordered ionic materials.[62] This process involves a hopping motion over few ionic diameters[26] and has been suggested to play a key role in ionic transport and thus in the systems' conductivity.[35,59,60,63] Since the population balance between strongly and weakly bound counterions is, in fact, dynamic in nature,[30,31] it is straightforward to assume that this mechanism works toward promoting the exchange between the two populations. A typical method for the identification of such a process is through the detection of a dynamic contrast between the examined particles; such a contrast can be inferred from the development of different peaks in their self-Van Hove function,[53,54] as is the case in our systems (Figs. 5 and 6). The dynamic exchange process between the counterions belonging to the condensed and to the loose shell around the dendrimer in the strong electrostatic regime might be responsible for the dendrimer size dependence of the $C(t)$ relaxation times noted in Fig. 10. This can be understood through a coupling between this process and the rotational motion of the dendrimer, which, in dilute solutions, is faster than the dendrimer diffusion and bares molecular-size dependence.[43]

VIII. SUMMARY/CONCLUSIONS

In this work we have explored characteristics of counterions' motion in a dilute solution of peripherally charged dendrimer molecules (in a UA representation) with the presence of explicit solvent beads, under the influence of different strengths of electrostatic interactions. Models of two different dendrimer sizes (i.e., of the third and the fourth generation) and two different concentrations (in the dilute regime) of the solute were examined.

Different dynamic probes were utilized in order to study dynamic aspects of counterion motion at different length and time scales. In the long-time limit, and in the range of electrostatic interactions where the degree of counterion condensation was significant (i.e., at l_B/σ values ≥ 10 when the percentage of the condensed counterions was 60% or higher[13]), the diffusive motion of counterions was essentially coupled to that of the dendrimer molecules. The diffusion coefficients of both, the counterion and the dendrimer species, were found to follow a common power-law dependence on Bjerrum length with an exponent close to -3. This motional coupling between condensed counterions and dendrimers in the strong Coulombic regime was consistent with the manifestation of a dynamic transition in the survival (residence) times of the pairs formed between counterions and dendrimer charged beads, much in analogy to the observed coupling between counterions and long length scale dynamic modes in other macromolecular electrolyte systems.[10,30,64,65] In the weak electrostatic regime where the majority of counterions are only loosely associated with the charged dendrimer beads, the relevant residence time scale is much shorter; in this regime these counterions can be visualized to perform an oscillatory motion along the direction of loose virtual bonds connecting them with the charged dendrimer beads, in a fashion similar to the motion characterized as the "high frequency" process in dielectric relaxation experiments performed in polyelectrolyte solutions.[32] This process appears to be coupled to global dendrimer motion as well, most probably through the dendrimer rotational relaxation.

In the strong electrostatic regime, we can also monitor the dynamic behavior of those counterions not tightly bound to the charged dendrimer beads. Dynamics of these counterions, although referring to a rather low percentage of the total population, may be important in applications where ion transport is desired to be carefully controlled.[64,66] As has been demonstrated in our analysis of Van Hove functions in the latter regime, the time scale at which populations with noticeably different mobilities appear, as well as the time scale for relaxation of local counterion density fluctuations, is much shorter compared to the residence times of the strongly bound counterions. This information, combined with the structural details concerning the arrangement of counterions (either around the charged dendrimer beads or around other counterions), indicated that the dynamic features observed in the distinct and the self-part of the Van Hove functions were mainly related to the population of counterions loosely bound to the dendrimers and to the exchange mechanism between them and the condensed population, respectively. The time scale for the decay of the collective modes characterizing the loosely bound population was found to be moderately longer compared to that for the development of a mobility contrast between individual counterions. This collective motion was also found to be dendrimer size dependent, which indicates a coupling with global dendrimer dynamics. The time scale for the collective motion was found to range between 10τ and 100τ depending on the strength of electrostatic interactions.

If we would like to map the simulation time to real units, assigning the unit length $\sigma \cong 3.3$ Å as was shown in our previous work[13] and taking $\varepsilon=0.3k_BT$ as has been considered for the energy simulation units,[13] τ would correspond to approximately 1.4 ps at room temperature. From light scattering experiments in highly charged (salt-free) polyelectrolyte

solutions,[67] it was found that the diffusion coefficient extracted from a dynamic process associated with the coupled counterion-polyion motion and in a wide concentration range was between 10^{-5} and 10^{-6} cm^2/s for monovalent counterions. For divalent counterions, inelastic x-ray measurements[4] yielded a diffusion coefficient for bound counterions close to 5×10^{-4} cm^2/s. Mapping the units of length and time to real units as discussed above, we calculate that between $l_B/\sigma=10$ and $l_B/\sigma=60$ the diffusion coefficient of the counterions (Fig. 3) varies between 10^{-4} and 10^{-6} cm^2/s which captures the order of magnitude observed in the relevant experiments. Moreover, in electron paramagnetic resonance measurements including systems with low ionic strength (i.e., with virtually unscreened Coulombic interactions) and at different concentrations[30,31] showed that the lifetime of contact between counterions and polyelectrolyte chains as well as that associated with the exchange between territorially bound and "free" counterions corresponds to a subnanosecond time scale. This is consistent with the time scales found either for the appearance of a second peak in the self-Van Hove function (ranging from 10τ to 100τ for the examined models, Figs. 6 and 7) or for the average residence times of counterions as illustrated in Fig. 12.

In conclusion, we believe that the results described in the present work elucidate essential characteristics of the dynamics of counterions and provide a more detailed account for the study of ion migration phenomena in dilute polyelectrolyte solutions and under the influence of different strengths of electrostatic interactions.

ACKNOWLEDGMENTS

Funding from the Greek General Secretariat for Research and Technology and the European Community under the framework of the PENED 2003 program (Grant No. 03EΔ716) is gratefully acknowledged.

[1] M. Mandel, in *Encyclopedia of Polymers Science and Engineering*, edited by H. F. Mark (Wiley, New York, 1985).
[2] J. R. C. Vandermaarel, L. C. A. Groot, J. G. Hollander, W. Jesse, M. E. Kuil, J. C. Leyte, L. H. Leytezuiderweg, M. Mandel, J. P. Cotton, G. Jannink, A. Lapp, and B. Farago, Macromolecules **26**, 7295 (1993).
[3] S. Sen, L. A. Gearheart, E. Rivers, H. Liu, R. S. Coleman, C. J. Murphy, and M. A. Berg, J. Phys. Chem. B **110**, 13248 (2006).
[4] T. E. Angelini, R. Golestanian, R. H. Coridan, J. C. Butler, A. Beraud, M. Krisch, H. Sinn, K. S. Schweizer, and G. C. L. Wong, Proc. Natl. Acad. Sci. U.S.A. **103**, 7962 (2006).
[5] K. Andresen, R. Das, H. Y. Park, H. Smith, L. W. Kwok, J. S. Lamb, E. J. Kirkland, D. Herschlag, K. D. Finkelstein, and L. Pollack, Phys. Rev. Lett. **93**, 248103 (2004).
[6] R. Das, T. T. Mills, L. W. Kwok, G. S. Maskel, I. S. Millett, S. Doniach, K. D. Finkelstein, D. Herschlag, and L. Pollack, Phys. Rev. Lett. **90**, 188103 (2003).
[7] F. J. M. Schipper, J. G. Hollander, and J. C. Leyte, J. Phys.: Condens. Matter **10**, 9207 (1998).
[8] D. Hinderberger, H. W. Spiess, and G. Jeschke, J. Phys. Chem. B **108**, 3698 (2004).
[9] J. Appell, G. Porte, and E. Buhler, J. Phys. Chem. B **109**, 13186 (2005).
[10] T. E. Angelini, H. Liang, W. Wriggers, and G. C. L. Wong, Proc. Natl. Acad. Sci. U.S.A. **100**, 8634 (2003).
[11] T. S. Lo, B. Khusid, and J. Koplik, Phys. Rev. Lett. **100**, 128301 (2008).
[12] S. Pappalardo, V. Villari, S. Slovak, Y. Cohen, G. Gattuso, A. Notti, A. Pappalardo, I. Pisagatti, and M. R. Parisi, Chem.-Eur. J. **13**, 8164 (2007).
[13] K. Karatasos, Macromolecules **41**, 1025 (2008).
[14] A. Stradner, H. Sedgwick, F. Cardinaux, W. C. K. Poon, S. U. Egelhaaf, and P. Schurtenberger, Nature (London) **432**, 492 (2004).
[15] P. K. Maiti and B. Bagchi, Nano Lett. **6**, 2478 (2006).
[16] X. Qiu, K. Andresen, L. W. Kwok, J. S. Lamb, H. W. Park, and L. Pollack, Phys. Rev. Lett. **99**, 038104 (2007).
[17] N. Ise, T. Konishi, and B. V. R. Tata, Langmuir **15**, 4176 (1999).
[18] M. Deserno, F. Jimenez-Angeles, C. Hohn, and M. Lozada-Cassou, J. Phys. Chem. B **105**, 10983 (2001).
[19] M. Quesada-Perez, J. Callejas-Fernandez, and R. Hidalgo-Alvarez, Adv. Colloid Interface Sci. **95**, 295 (2002).
[20] L. F. Rojas-Ochoa, R. Castaneda-Priego, V. Lobaskin, A. Stradner, F. Scheffold, and P. Schurtenberger, Phys. Rev. Lett. **100**, 178304 (2008).
[21] D. Gottwald, C. N. Likos, G. Kahl, and H. Löwen, Phys. Rev. Lett. **92**, 068301 (2004).
[22] V. M. Prabhu, E. J. Amis, D. P. Bossev, and N. Rosov, J. Chem. Phys. **121**, 4424 (2004).
[23] I. Morfin, F. Horkay, P. J. Basser, F. Bley, A.-M. Hecht, C. Rochas, and E. Geissler, Biophys. J. **87**, 2897 (2004).
[24] A. Popov and D. A. Hoagland, J. Polym. Sci., Part B: Polym. Phys. **42**, 3616 (2004).
[25] W. K. Kim and W. Sung, Phys. Rev. E **78**, 021904 (2008).
[26] R. Chang and A. Yethiraj, J. Chem. Phys. **116**, 5284 (2002).
[27] T. E. Angelini, L. K. Sanders, H. J. Liang, W. Wriggers, J. X. Tang, and G. C. L. Wong, J. Phys.: Condens. Matter **17**, S1123 (2005).
[28] F. Bordi, C. Cametti, and R. H. Colby, J. Phys.: Condens. Matter **16**, R1423 (2004).
[29] Y. Katsumoto, S. Omori, D. Yamamoto, A. Yasuda, and K. Asami, Phys. Rev. E **75**, 011911 (2007).
[30] D. Hinderberger, H. W. Spiess, and G. Jeschke, Macromol. Symp. **211**, 71 (2004).
[31] D. Hinderberger, G. Jeschke, and H. W. Spiess, Macromolecules **35**, 9698 (2002).
[32] J. Oizumi, Y. Kimura, K. Ito, and R. Hayakawa, Colloids Surf., A **145**, 101 (1998).
[33] N. Ookubo, I. Teraoka, and R. Hayakawa, Ferroelectrics **86**, 19 (1988).
[34] H. Washizu and K. Kikuchi, J. Phys. Chem. B **110**, 2855 (2006).
[35] C. Reznik, Q. Darugar, A. Wheat, T. Fulghum, R. C. Advincula, and C. F. Landes, J. Phys. Chem. B **112**, 10890 (2008).
[36] A. A. Gurtovenko, S. V. Lyulin, M. Karttunen, and I. Vattulainen, J. Chem. Phys. **124**, 094904 (2006).
[37] Y. Rabin and M. Tanaka, Phys. Rev. Lett. **94**, 148103 (2005).
[38] F. J. M. Schipper, K. Kassapidou, and J. C. Leyte, J. Phys.: Condens. Matter **8**, 9301 (1996).
[39] C. Devadoss, P. Bharathi, and J. S. Moore, Angew. Chem., Int. Ed. Engl. **36**, 1633 (1997).
[40] A. Topp, B. J. Bauer, D. A. Tomalia, and E. J. Amis, Macromolecules **32**, 7232 (1999).
[41] A. Bonincontro, C. Cametti, B. Nardiello, S. Marchetti, and G. Onori, Biophys. Chem. **121**, 7 (2006).
[42] H. M. Harreis, C. N. Likos, and M. Ballauff, J. Chem. Phys. **118**, 1979 (2003).
[43] K. Karatasos, D. B. Adolf, and G. R. Davies, J. Chem. Phys. **115**, 5310 (2001).
[44] S. L. Mayo, B. D. Olafson, and W. A. Goddard III, J. Phys. Chem. **94**, 8897 (1990).
[45] K. Binder, J. Baschnagel, and W. Paul, Prog. Polym. Sci. **28**, 115 (2003).
[46] K. A. Dawson, Curr. Opin. Colloid Interface Sci. **7**, 218 (2002).
[47] K. Karatasos, Macromolecules **39**, 4619 (2006).
[48] M. Tokuyama, Phys. Rev. E **58**, R2729 (1998).
[49] J.-P. Hansen and I. R. McDonald, *Theory of Simple Liquids*, 3rd ed. (Elsevier, Amsterdam, 2006).
[50] H. E. Fischer, A. C. Barnes, and P. S. Salmon, Rep. Prog. Phys. **69**, 233 (2006).
[51] W. Kob, C. Donati, S. J. Plimpton, P. H. Poole, and S. C. Glotzer, Phys. Rev. Lett. **79**, 2827 (1997).
[52] F. Faupel, F. Werner, M.-P. Macht, H. Mehrer, V. Naundorf, K. Raetzke, H. Schober, D. Sharma, and H. Teichler, Rev. Mod. Phys. **75**, 237 (2003).
[53] J. Habasaki, K. L. Ngai, and Y. Hiwatari, Phys. Rev. E **66**, 021205 (2002).
[54] E. G. Kim and W. L. Mattice, J. Chem. Phys. **117**, 2389 (2002).
[55] K. Karatasos and A. V. Lyulin, J. Chem. Phys. **125**, 184907 (2006).
[56] J. Pinero, L. B. Bhuiyan, J. Rescic, and V. Vlachy, J. Chem. Phys. **127**, 104904 (2007).
[57] D. Swiatla-Wojcik, Chem. Phys. **342**, 260 (2007).

[58] See EPAPS Document No. E-JCPSA6-130-023910 for pair distribution function between charged dendrimer beads and counterions in one of the studied models. The vertical line denotes the cutoff distance. The pair distribution functions of all the other examined models are in complete analogy, therefore the same cutoff value has been adopted for the rest of the systems as well. For more information on EPAPS, see http://www.aip.org/pubservs/epaps.html.
[59] S. T. Cui, Phys. Rev. Lett. **98**, 138101 (2007).
[60] N. Ramesh and J. L. Duda, J. Membr. Sci. **191**, 13 (2001).
[61] M. C. Lonergan, A. Nitzan, M. A. Ratner, and D. F. Shriver, J. Chem. Phys. **103**, 3253 (1995).
[62] K. Funke and R. D. Banhatti, Solid State Sci. **10**, 790 (2008).
[63] V. Kytin, T. Dittrich, J. Bisquert, E. A. Lebedev, and F. Koch, Phys. Rev. B **68**, 195308 (2003).
[64] R. E. A. Dillon and D. F. Shriver, Chem. Mater. **13**, 1369 (2001).
[65] V. M. Prabhu, Curr. Opin. Colloid Interface Sci. **10**, 2 (2005).
[66] R. N. Barnett, C. L. Cleveland, A. Joy, U. Landman, and G. B. Schuster, Science **294**, 567 (2001).
[67] Y. B. Zhang, J. F. Douglas, B. D. Ermi, and E. J. Amis, J. Chem. Phys. **114**, 3299 (2001).